The following publication Guoqing Zhang and Suet To "Cutting force modelling of ultra-precision flycutting of groove", Proc. SPIE 10838, 9th International Symposium on Advanced Optical Manufacturing and Testing Technologies: Advanced Optical Manufacturing Technologies, 1083819 (16 January 2019) is available at https://doi.org/10.1117/12.2505813.

Cutting force modelling of ultra-precision fly cutting of groove

Guoqing Zhang[a], Suet To[*b]
[a]Guangdong Provincial Key Laboratory of Micro/Nano Optomechatronics Engineering, College of Mechatronics and Control Engineering, Shenzhen University, Nan-hai Ave 3688, Shenzhen, Guangdong, PR China 518060; [b]State Key Laboratory of Ultra-precision Machining Technology, Department of Industrial and Systems Engineering, The Hong Kong Polytechnic University, Kowloon, Hong Kong, PR China

ABSTRACT

Cutting force is a key factor of the cutting plans design, cutting conditions setting, tool wear evaluation and even machined surface topography prediction. However, little research has been conducted on the analysis of cutting force in ultra-precision fly cutting (UPFC). This paper presents a theoretical and experimental study on the cutting force modelling in UPFC of groove. In the present study, an analytic cutting force model has been established to predict the cutting force amplitudes both in the feed direction and thrust direction. Experiments were conducted to verify the simulation results. Theoretical and experimental results show that cutting force in UPFC is figured as a force pulse followed by a series of free vibration signals, cutting parameters such as cutting depth, feed rate seriously affect cutting force amplitude.

Keywords: Ultra-precision fly cutting, cutting force, modelling, groove

1. INTRODUCTION

Ultra-precision fly cutting (UPFC) is a crucial method for producing non-rotational symmetric optical surface structures with micrometric form accuracy and nanometric surface finish[1-2]. Differs from turning process, cutting tool rotates during UPFC; differs from traditional milling process, only one tool tooth participate cutting in UPFC. Since the rotation speed of cutting tool is high in UPFC, the contact between diamond tool and workpiece is quite short[3]. Therefore, cutting force models for conventional turning or milling cannot be directly used in UPFC. The analysis of cutting force in UPFC is quite important, a good understanding of the cutting force generation is the key step to understand the cutting mechanism of UPFC[4]. Until now, quite a lot of researchers paid their attention to the development of an accurate tool force model in single point diamond turning, conventional turning process and other continuous cutting process. Merchant presented a comprehensive orthogonal tool force model[5], whose model could predict the tool forces under different cutting parameters (rake angle, shear angle, material, etc.). However, Merchant failed to consider material spring back effect in his model. Afterwards, researchers start to concern the effect of material spring back in the machined surface and their rebound force to the clearance face of diamond tools[6-8]. However, due to the intermittent cutting process and short cutting time of UPFC, it is difficult to build up a model to predict the cutting force for UPFC. Until now, little practical cutting force model for UPFC has been found in literature review.

This paper developed a theoretical and experimental study on cutting force modelling of UPFC of groove. Based on the Merchant's tool force model and the cutting mechanism of UPFC, this research developed a cutting force model for UPFC of groove. This model could predict the cutting force component both in the feed direction and thrust direction. This research is potentially used to explore the fundamental of material slide, shear deformation, material spring back and chip generation in UPFC of groove.

2. EXPERIMENTAL SETUP

In this research, two grooves were machined, cutting parameters employed in the present research are shown in table 1. The workpiece is coper material, cutting environment is lubricant on. In the experiment, cutting force signal was

* sandy.to@polyu.edu.cn; phone +86-755-22673853; fax +86- 755-26557471.

AOMATT 2018: Advanced Optical Manufacturing Technologies, edited by Xiong Li, William T. Plummer, Bin Fan, Mingbo Pu, Yongjian Wan, Xiangang Luo, Proc. of SPIE Vol. 10838, 1083819
© 2019 SPIE · CCC code: 0277-786X/19/$18 · doi: 10.1117/12.2505813

captured first by the sensor of Kistler 9256C1 dynamometer and amplified by Kistler 5080A charge amplifier and then A/D conversed by Kistler 5697A2 DAQ-System, at last the signal was figured and analyzed by the dynamometer attached software-Dynaware.

Table 1. Cutting parameters used in this experiment.

Items	V1 value	V2 value
Tool type	APEX Insert Diamond tool	
Rake angle	-2.5°	
Clearance angle	15°	
Tool radius	0.631mm	
Feed rate	200mm/min	300 mm/min
Spindle speed	4500 rpm	1500rpm
Depth of cut	0.02mm	0.05mm
Swing distance	Around 25mm	Around 25mm
Groove depth	0.5mm(25layers)	0.5mm(10layers)

3. CUTTING FORCE MODELLING

In UPFC process, although diamond tools fly and cut workpiece intermittently, UPFC is a continuous cutting process on a microscopic scale. The continuous process on a microscopic scale is schematically illustrated in Figure 1, where γ is the rake angle of diamond tools, ϕ is the shear angle.

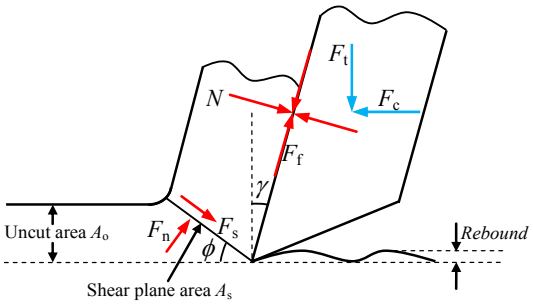

Figure 1. Schematic illustration of force components in a continuous cutting process

In the present research, the used material failure criteria is Von Mises criterion, based on this criterion, the shear stress on the shear plane is expressed as $\tau_s = H/3\sqrt{3}$. The cutting process is an isothermal and adiabatic process.

According to Figure 1, the cutting force components in feed direction and thrust direction are derived as:

$$\begin{aligned} F_c &= F_s \cos\phi + F_n \sin\phi \\ F_t &= F_n \cos\phi - F_s \sin\phi \end{aligned} \tag{1}$$

Where F_c and F_n are the force components along the shear plane and normal to the shear plane. On the shear plane, the normal stress is expressed as $\sigma_s = H/3$[6], therefore the force component normal to the shear plane is:

$$F_n = \sigma_s A_s = \frac{H}{3}\frac{A_o}{\sin\phi} \tag{2}$$

Where H is the Viker's hardness of the workpiece materials, A_s is the area of the shear plane, A_o is the uncut area.

Since the shear stress on the shear plane is expressed as $\tau_s = H/3\sqrt{3}$ [6], the shear force on the shear plane is expressed as:

$$F_s = \tau_s A_s = \tau_s \frac{A_o}{\sin\phi} = \frac{H}{3\sqrt{3}}\frac{A_o}{\sin\phi} \tag{3}$$

Therefore, according to Eq.(2)-(3), Eqs.(1) is expressed as:

$$F_c = \frac{H}{3}\frac{A_o}{\sin\phi}\left(\frac{\cos\phi}{\sqrt{3}}+\sin\phi\right)$$
$$F_t = \frac{H}{3}\frac{A_o}{\sin\phi}\left(\cos\phi-\frac{\sin\phi}{\sqrt{3}}\right) \tag{4}$$

Based on Eqs.(4), cutting force both in feed direction and thrust direction depend on the uncut area A_0.

The chip formation in UPFC is schematic illustrated in Figure 2, the uncut chip is enveloped by the trajectory of the last fly cutting, the present fly cutting and uncut workpiece surface. At different rotation position (e.g. angle α), the chip thickness is also different, there exists a crucial angle θ, who divides the chip area into two sections, this crucial angle is derived as:

$$\theta = arc\tan\frac{\sqrt{2S_w a_p - a_p^2} - f_e}{S_w - a_p} \tag{5}$$

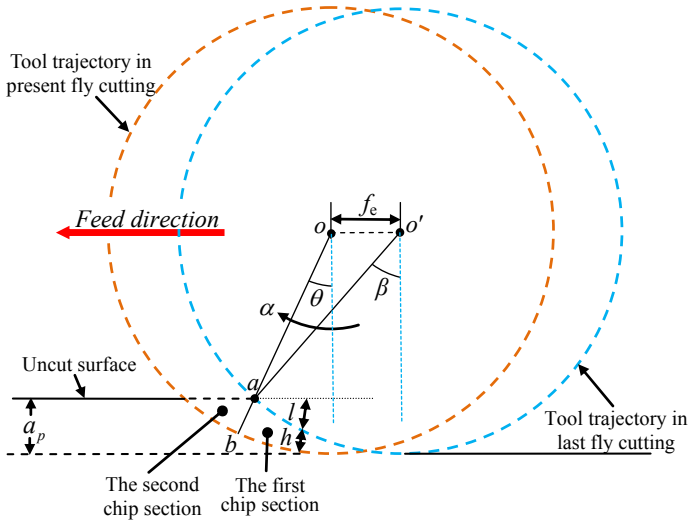

Figure 2. Schematic illustration of cutting and chip formation process in UPFC

As $0 \le \alpha \le \theta$, diamond tool locates at the first chip section, In this section, the chip is enveloped by the trajectory of the last fly cutting, the present fly cutting and uncut workpiece surface, whose cross section profile is schematic illustrated in Figure 3(a), in Figure 3, angles ψ and ζ are derived as:

$$\begin{cases} \psi = \arccos\left(\dfrac{R-l}{R}\right) \\ \xi = \arccos\left(\dfrac{R-l-h}{R}\right) \end{cases} \tag{6}$$

Where A_1 and A_2 in Figure 3(a) are the areas of two round segments, derived as:

$$\begin{cases} A_1 = \psi R^2 - \dfrac{R(R-l)\sin\psi}{2} \\ A_2 = \xi R^2 - \dfrac{R(R-l-h)\sin\xi}{2} \end{cases} \tag{7}$$

The area of the chip's cross section is derived as:

$$A_o = A_2 - A_1 = (\xi-\psi)R^2 + \frac{R(R-l)}{2}(\sin\psi-\sin\xi) + \frac{Rh\sin\xi}{2} \tag{8}$$

Where $h = f \sin\alpha$ is the chip thickness, $l = R - \dfrac{R - a_p}{\cos\alpha}$ is the previous cutting depth.

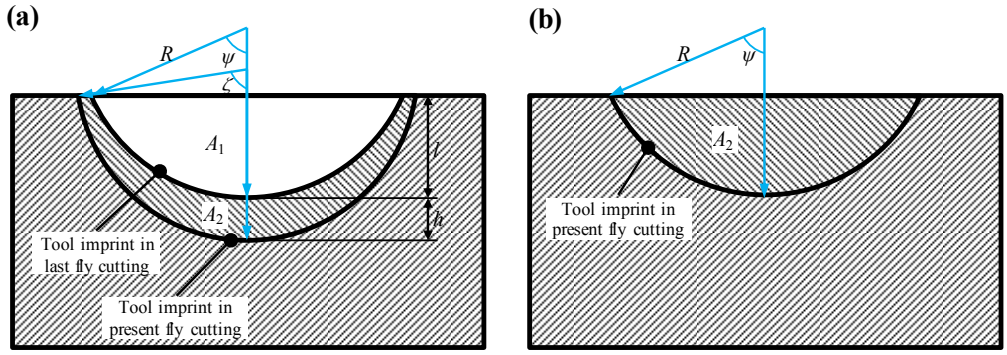

Figure 3. Cross section of the chip when (a) $0 \le \alpha \le \theta$ and (b) $\theta \le \alpha \le \beta$

As $\theta < \alpha \le \beta$, diamond tool locates at the second chip section. In this section, the chip is enveloped by the tool imprint of the present fly cutting and the uncut surface, as is shown in Figure 3(b). The area of the chip's cross section is derived as:

$$A_o = A_1 = \psi R^2 - \frac{R(R-l)\sin\psi}{2} \tag{9}$$

According to Eqs.(4,8-9), cutting force components in feed direction and thrust direction depend on the rotation angle α as other constants are determined. However, dynamometer used in this experiment can merely capture the horizontal and vertical force components. Therefore, the force components need to transfer to the force components in horizontal and vertical directions. The schematic illustration of horizontal and vertical force components in UPFC is shown in Figure 4, while the calculation formula is derived as:

$$\begin{aligned} F_x &= F_h = F_t \sin\alpha + F_c \cos\alpha \\ F_z &= -F_v = F_c \sin\alpha - F_t \cos\alpha \end{aligned} \tag{10}$$

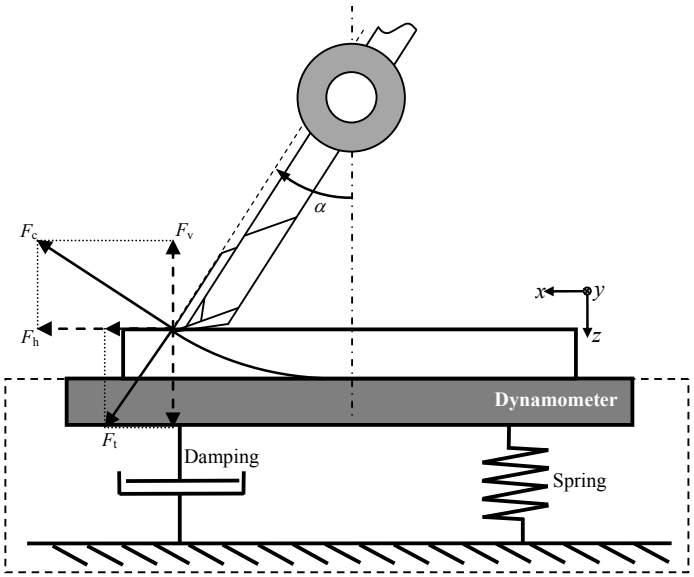

Figure 4. Schematic illustration of cutting force components in horizontal and vertical direction

In this paper, coper was chosen as workpiece material, whose hardness and elastic modulus are measured as 145HV and 0.95×10^5 MPa respectively. Through the MATLAB simulation program, the simulated cutting force pulse is drawn in Figure 5.

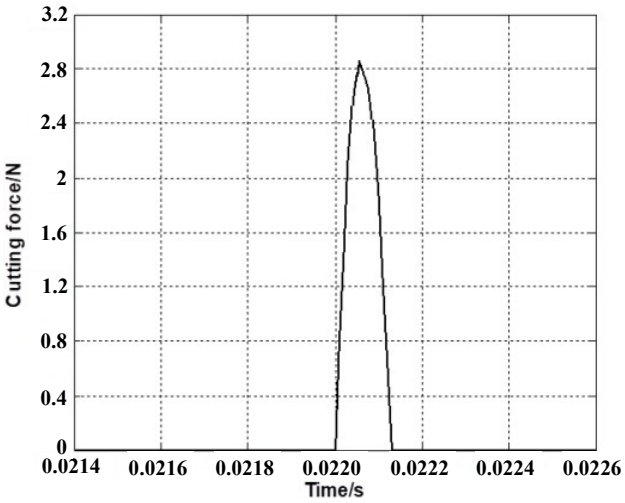

Figure 5. Simulated cutting force pulse for UPFC

The simulated cutting force indicates that the duration of cutting force is quite short, as the diamond tool cut into and out of the workpiece surface, the amplitude of cutting force increases first and then decreases quickly. Thus, the exhibition of cutting force for UPFC is figured as a force pulse.

4. EXPERIMENTAL VERIFICATION

In the present research, cutting force was captured and analyzed by the Dynamometer attached software. The original cutting force in three channels are shown in Figure 6, in Figure 6, section A is the air cutting process, therefore the force amplitude is quite small and mixed by the background noise. While section B is the cut-in section, in this section, the cutting force increases to the regular amplitude with the completing of the cutting. Section C is the complete cutting section, in this section, cutting force reflects cutting energy of the chip formation.

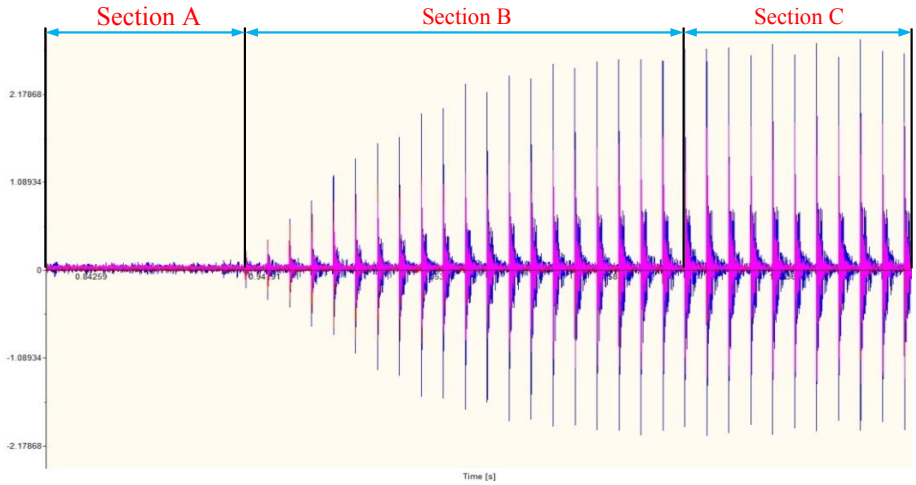

Figure 6. Cutting force in different cutting stage

The cutting force forms in a rotary cutting of UPFC is shown in Figure 7, the first pulse is the cutting force, the followed signal is the free vibration signal stimulated by the force pulse. According to the comparison of the captured cutting force and simulated one, it is found that the cutting force model could be used to simulate the cutting force in UPFC.

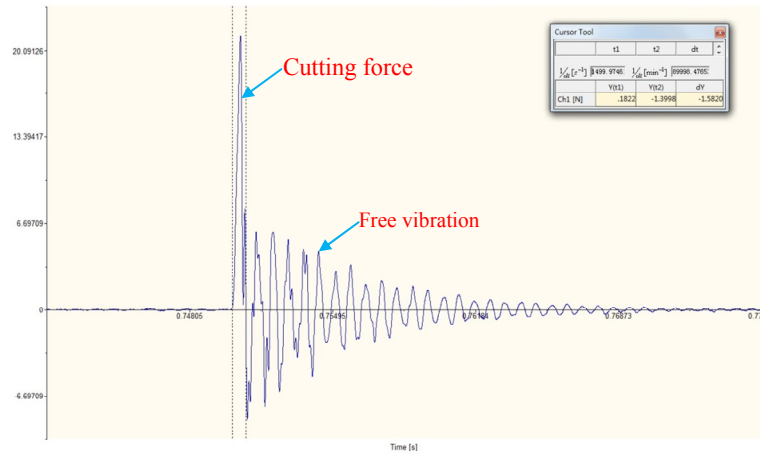

Figure 7. Cutting force composition

Also, cutting experiments under different cutting parameters found that cutting parameters seriously affect the cutting force amplitude. Both the theoretical and experimental results show that cutting force increases with the growing of cutting depth and feed rate.

5. CONCLUSION

By combining the cutting mechanism of UPFC and the Merchant' tool force model, a cutting force model for UPFC of groove is derived. The model could be used to calculate and predict cutting force both in feed direction and thrust direction. Also, a serious of cutting experiments were conducted to explore the relationship between cutting parameters and cutting force amplitude. Experimental and simulated results reflected that captured cutting force agrees well with the simulated one although deviation were existed due to the noise and impact load of UPFC, and cutting force increases with the growing of depth of cut and feed rate.

ACKNOWLEDGEMENTS

This research was supported by the National Natural Science Foundation of China (Grant No. 51505297), the Natural Science Foundation of Guangdong Province (Grant No. 2017A030313295), the Shenzhen Science and Technology Program (Grant No. JCYJ20160422170026058), the Shenzhen Peacock Technology Innovation Project (Grant No. KQJSCX20170727101318462), the Shenzhen University Teaching Reform Project (JG2017063) and the Shenzhen University Graduate "Exemplary Seminar Course".

REFERENCES

[1] Cheung, C.F., Kong, L.B., Lee, W.B., et al., "Modelling and simulation of freeform surface generation in ultra-precision raster milling," Proceedings of the Institution of Mechanical Engineers Part B Journal of Engineering Manufacture 220(11), 1787-1801 (2006).

[2] Lee, W.B., "Ultra-precision Machining Technique for Optical Free-surface and Its Application," Manufacturing Technology & Machine Tool, 2004.

[3] Zhang, G., To, S., Xiao. G., "The relation between chip morphology and tool wear in ultra-precision raster milling," International Journal of Machine Tools & Manufacture 80–81(4),11-17 (2014).

[4] To, S., Zhang, G., "Study of cutting force in ultra-precision raster milling of V-groove," International Journal of Advanced Manufacturing Technology 75(5-8), 967-978 (2014).

[5] Merchant, M.E., "Mechanics of the metal cutting process. I: orthogonal cutting and a type 2 chip," Journal of Applied Physics 16, 267–275 (1945).

[6] J. Drescher D., Tool force, tool edge and surface finish relationships in diamond turning: [PhD Dissertation], Raleigh: North Carolina State University, (1992).
[7] Foe, L.A., Dautzenberg, J.H. and Vander Wolf, A.C.H., "Cutting forces and their influences upon the surface integrity in single-point diamond turning," Proceedings of the International Congress for Ultraprecision Technology 110–125 (1988).
[8] Kang, I.S., Kim, J.S., Kim, J.H., "A mechanistic model of cutting force in the micro end milling process," Materials Processing Technology 187-188, 250-255 (2007).